Journal of Experimental Botany, Vol. 67, No. 22 pp. 6337–6349, 2016
doi:10.1093/jxb/erw401 Advance Access publication 2 November 2016

RESEARCH PAPER

Nitrite is the driver, phytohormones are modulators while NO and H_2O_2 act as promoters of NO_2-induced cell death

Dörte Kasten[1], Axel Mithöfer[2], Elisabeth Georgii[1], Hans Lang[3], Jörg Durner[1] and Frank Gaupels[1,*]

[1] Institute of Biochemical Plant Pathology, Helmholtz Zentrum München, German Research Center for Environmental Health, Ingolstädter Landstraße 1, D-85764 Neuherberg, Germany
[2] Max Planck Institute for Chemical Ecology, Department Bioorganic Chemistry, Hans-Knöll-Straße 8, D-07745 Jena, Germany
[3] Research Unit Environmental Simulation, Helmholtz Zentrum München, German Research Center for Environmental Health, Ingolstädter Landstraße 1, D-85764 Neuherberg, Germany

* Correspondence: frank.gaupels@helmholtz-muenchen.de

Received 9 August 2016; Editorial decision 7 October 2016; Accepted 7 October 2016

Editor: Peter Bozhkov, Swedish University of Agricultural Sciences

Abstract

This study aimed to understand the molecular mechanisms of nitrogen dioxide (NO_2)-induced toxicity and cell death in plants. Exposure of Arabidopsis to high concentrations of NO_2 induced cell death in a dose-dependent manner. No leaf symptoms were visible after fumigation for 1 h with 10 parts per million (ppm) NO_2. However, 20 ppm NO_2 caused necrotic lesion formation and 30 ppm NO_2 complete leaf collapse, which had already started during the 1 h fumigation period. NO_2 fumigation resulted in a massive accumulation of nitrite and in protein modifications by *S*-nitrosylation and tyrosine nitration. Nitric oxide (NO) at 30 ppm did not trigger leaf damage or any of the effects observed after NO_2 fumigation. The onset of NO_2-induced cell death correlated with NO and hydrogen peroxide (H_2O_2) signaling and a decrease in antioxidants. NO- and H_2O_2-accumulating mutants were more sensitive to NO_2 than wild-type plants. Accordingly, experiments with specific scavengers confirmed that NO and H_2O_2 are essential promoters of NO_2-induced cell death. Leaf injection of 100 mM nitrite caused an increase in *S*-nitrosylation, NO, H_2O_2, and cell death suggesting that nitrite functioned as a mediator of NO_2-induced effects. A targeted screening of phytohormone mutants revealed a protective role of salicylic acid (SA) signaling in response to NO_2. It was also shown that phytohormones were modulators rather than inducers of NO_2-induced cell death. The established experimental set-up is a suitable system to investigate NO_2 and cell death signaling in large-scale mutant screens.

Key words: Antioxidative system, cell death, H_2O_2, NO, NO_2, nitrite, phytohormones, *S*-nitrosothiols, tyrosine nitration.

Introduction

The gaseous free radical NO regulates adaptive responses to salt, drought, ozone, and various other abiotic stress encounters (Fancy *et al.*, 2016). Additionally, NO has a prominent role in plant defense responses during plant–pathogen interactions (Durner *et al.*, 1998; Gaupels *et al.*, 2011; Mur *et al.*, 2013). During incompatible interactions the endogenous production of NO and reactive oxygen species (ROS) triggers a hypersensitive response (HR) synergistically since neither ROS nor NO alone is capable of triggering an advanced HR (Delledonne *et al.*, 1998; Leitner *et al.*, 2009; Scheler *et al.*, 2013; Wang *et al.*, 2013). Salicylic acid (SA), ethylene, NO, and ROS amplify each other in a feedforward mechanism promoting cell death propagation (Leon *et al.*, 1995; Mur *et al.*, 2008). By contrast, jasmonic acid (JA) accumulation

is involved in the containment of cell death propagation as shown after acute ozone exposure (Overmyer *et al.*, 2000; Rao *et al.*, 2000).

Nitrite reduction by nitrate reductase (NR) and arginine oxidation by nitric oxide synthase (NOS)-like enzymes are major NO sources during plant stress responses (Besson-Bard *et al.*, 2008). ROS are mainly produced by the NADPH oxidases REACTIVE BURST OXIDASE HOMOLOG D and F (RBOHD and F) (Torres and Dangl, 2005; Gilroy *et al.*, 2014). The production of ROS is confined by the antioxidative system including the redox couples ascorbate (AsA)–dehydroascorbate (DHA) and glutathione (GSH)–glutathione disulfide (GSSG). By enzymatic oxidation and reduction of these antioxidants, the cellular redox balance is guaranteed and oxidative damage is avoided (Noctor and Foyer, 1998). Antioxidants also interact with NO and its derivatives to regulate their cellular abundance and thereby prevent nitrosative stress (Groß *et al.*, 2013). For instance, GSH can be converted to *S*-nitrosoglutathione (GSNO) by binding NO, and thereby functions as an endogenous NO shuttle and store. NO homeostasis is indirectly controlled by the GSNO-degrading enzyme GSNO reductase (GSNOR) (Yu *et al.*, 2014).

Due to its radical nature, NO is able to form a multitude of oxo-derivatives when reacting with ROS such as superoxide (O_2^-) or hydrogen peroxide (H_2O_2) (Table 1). Collectively, these are known as reactive nitrogen species (RNS). Amongst others, RNS encompass the nitrosonium cation (NO^+) and the nitroxyl anion (NO^-), as well as higher oxides of NO such as peroxynitrite ($ONOO^-$), dinitrogen trioxide (N_2O_3) and nitrogen dioxide (NO_2) (Groß *et al.*, 2013). NO and RNS confer their bioactivity through post-translational protein modifications causing conformational alterations that consequently lead to changes in protein activity. For instance, the covalent addition of a NO moiety to a reactive thiol group of cysteines leading to *S*-nitrosothiol (SNO) (Table 1) formation was shown to play central roles in the regulation of disease resistance and HR (Romero-Puertas *et al.*, 2008; Tada *et al.*, 2008; Lindermayr *et al.*, 2010; Yun *et al.*, 2011). Additionally, the nitration (addition of a NO_2 moiety) of tyrosine residues mediated by $ONOO^-$ and NO_2 is another regulatory protein modification during plant defense responses (Table 1) (Leitner *et al.*, 2009; Gaupels *et al.*, 2011; Begara-Morales *et al.*, 2016).

The gaseous RNS nitrogen dioxide (NO_2) is a product of the reaction of NO with molecular oxygen or ozone (Table 1). Over the past 50 years it has been occasionally reported that high (ppm) doses of exogenous NO_2 induced cell death in a number of plant species. For example, in 1966 necrosis formation was observed in pinto beans and *Nicotiana glutinosa* after exposure for several hours to NO_2 concentrations between 2 and 10 ppm (Taylor and Eaton, 1966). This is consistent with the description of severe leaf damage in *Nicotiana glutinosa* after fumigation with 5 ppm NO_2 for 1 h (Zeevaart, 1976). NO_2 hydrolyses within the aqueous environment of the cell to nitrate and nitrite, which are further converted to ammonium by the complementary action of nitrite and nitrate reductases (NR and NiR) (Beevers and Hageman, 1969; Crawford, 1995). The accumulation especially of nitrite is well known to cause plant injury (Mevius, 1958; Oke, 1966). Despite its toxicity, both nitrite and nitrate are described as being an important source of NO production (Besson-Bard *et al.*, 2008; Mur *et al.*, 2013).

NO_2 is produced in plant cellular metabolism by hemoglobins and peroxidases through one-electron oxidation of nitrite in the presence of H_2O_2 (Sakamoto *et al.*, 2004; Maassen and Hennig, 2011). Reports of elevated expression of hemoglobins during plant defense (Perazzolli *et al.*, 2006) and NO_2 emission from herbicide-treated plants (Klepper, 1979) are indicators of an involvement of NO_2 in the plant defense response. The reactive properties of the NO_2 radical predestine it to be a direct (nitration/oxidation) or indirect (conversion to other RNS) modifier of protein residues that may regulate signaling cascades during stress responses.

The aim of the present work was the detailed characterization of the NO_2-induced cell death in Arabidopsis. Short-term fumigation with high concentrations of NO_2 caused a strong increase of nitrite levels in leaf tissues. Both NO_2- and nitrite-induced cell death were dependent on the accumulation of H_2O_2 and NO. The involvement of phytohormones in the NO_2-induced cell death was implemented by hormone measurements and phenotypic mutant characterization upon NO_2 fumigation. Additionally, NO_2 fumigation is introduced as a useful non-invasive tool for investigating defense responses and cell death signaling in plants.

Table 1. *Selected chemical reactions of ROS and RNS*

ROS	RNS
Oxygen: O_2	Nitric oxide: $NO^{\cdot}$
Superoxide: $O_2^{\cdot-}$	Nitrogen dioxide: $NO_2^{\cdot}$
Hydrogen peroxide: H_2O_2	Dinitrogen trioxide: N_2O_3
Hydroxyl radical: $^{\cdot}OH$	Peroxynitrite: $ONOO^-$
ROS–RNS interactions	
$2\ NO^{\cdot} + O_2 \rightarrow 2\ NO_2^{\cdot}$	
$NO_2^{\cdot} + NO^{\cdot} \leftrightarrow N_2O_3$	
$NO^{\cdot} + O_2^- \rightarrow ONOO^-$	
$ONOO^- + H^+ \rightarrow NO_2^{\cdot} + {}^{\cdot}OH$	
Tyrosine nitration (not stoichiometric)	
Protein-Tyr + $^{\cdot}OH$ (or other radical) → Protein-Tyr$^{\cdot}$	
Protein-Tyr$^{\cdot}$ + $NO_2^{\cdot}$ → Protein-Tyr-NO_2	
***S*-Nitrosylation (not stoichiometric)**	
Protein-S-H + $NO^{\cdot}$ → Protein-S-NO	
GSH (glutathione) + $NO^{\cdot}$ → GSNO (*S*-nitrosoglutathione)	

Material and methods

Plant material and treatments

Arabidopsis thaliana ecotype Columbia-0 (Col-0) and various mutants were used in this work. A detailed description of the mutant lines can be found in Supplementary Table S1 at *JXB* online. Plants were grown on soil under long-day conditions (14 h light–10 h dark; 65–85 µmol m^{-2} s^{-1} light intensity; 20°C day/18°C night; 65–68% relative humidity) after vernalization

for 2 days at 4°C in the dark. Four- to five-week-old Col-0 plants were exposed to NO or NO_2 for 1 h in an air-tight fumigation chamber, while a control group was exposed to air. NO gas at 15% was diluted in air upstream of the fumigation chamber. NO_2 was generated by the reaction of 15% NO with 100% O_2 in a mixing chamber containing Raschig glass rings. The NO and NO_2 concentrations were adjusted by regulating the NO flux rate and the air flow into and out of the fumigation chamber. The concentrations of NO and NO_2 were monitored with an AC32M analyser of chemiluminescent oxides of nitrogen (Environnement S.A.). Additionally, leaves were infiltrated with 10 or 100 mM sodium nitrite ($NaNO_2$) or water (negative control) from their abaxial side using a 1 ml syringe without a needle.

Cell death assay

Tissue damage was quantified via electrolyte leakage. Whole rosettes were harvested immediately after fumigation. After rinsing with double distilled water (ddH_2O), each rosette was incubated in 30 ml ddH_2O under gentle agitation at room temperature (RT). At the indicated time points the water conductivity (μS cm^{-1}) was determined using a conductivity meter (GLM 020A, Greisinger Electronic). The sample conductivities measured at the indicated time points were normalized to their respective conductivities measured after freezing and reheating to RT (100% electrolyte leakage). In some experiments leaves were infiltrated with one of 500 μM 2-(4-carboxyphenyl)-4,4,5,5-tetramethylimidazoline-1-oxyl-3-oxide (cPTIO; Sigma-Aldrich), water (control), 100 U ml^{-1} catalase (CAT; Sigma-Aldrich) in 0.38 M potassium phosphate buffer pH 7, or phosphate buffer alone (control). After air-drying of the infiltrated leaves for 30 min, plants were fumigated with 30 ppm NO_2 for 1 h, followed by immediate electrolyte leakage measurements. For cell death quantification after nitrite injection, four leaves per plant were infiltrated as described above and subjected to electrolyte leakage measurements after air-drying for 1 h. Additionally, cell death was examined histochemically 24 h after treatment by Trypan Blue staining, as described earlier (Joo *et al.*, 2005). The leaves were mounted in 50% glycerol and photographed with a Nikon DC300.

Nitrite, S-nitrosothiol, nitrate, and nitrotyrosine measurements

Approximately 100 mg of plant material was harvested immediately after fumigation or 3 h after nitrite infiltration. After freezing in liquid nitrogen, the samples were homogenized twice for 10 s using a Silamat S6 tissue homogenizer (Ivoclar Vivadent) and 1.7–2.0 mm glass pearls (Roth). The homogenized leaf material was extracted in 500 μl 1× phosphate-buffered saline (PBS) and incubated on ice for 10 min followed by centrifugation for 10 min at 19 000 *g*. The protein content of the plant extract was determined using the Protein Assay Dye Reagent Concentrate (Bio-Rad). Nitrite, SNO, and nitrate contents were determined using the Sievers Nitric Oxide Analyzer NOA 280i (GE Power and Water, Analytix). Endogenous nitrite was reduced to gaseous NO by injection of leaf extracts into a reaction vessel containing trijodide solution (28.5 mM I_2, 66.9 mM KI in 77.7% acetic acid) at 30 °C. For SNO detection, endogenous nitrite was scavenged by adding 5% sulfanilamide (w/v, in 1 M HCl) at a dilution of 1:9 to the sample before injection into the trijodide solution. The total nitrogen content was measured using a vanadium chloride solution (50 mM VCl_3 in 0.8 M HCl) at 90°C. Peak area integration and calculation of concentrations based on $NaNO_2$ and $NaNO_3$ standards were performed using the Sievers NO Analysis Software. The concentration of nitrate in the sample was determined by subtracting nitrite and SNO from the total nitrogen content. Tyrosine nitration in 50 μl plant extracts was determined using the nitrotyrosine chemiluminescence detection assay kit (Merck Millipore) following the manufacturer's instructions. Chemiluminescence was detected with the Infinite M1000 Pro plate reader (Tecan).

NO and H_2O_2 detection

Intracellular NO was detected using diaminofluorescein-FM diacetate (DAF-FM DA; Sigma-Aldrich). Leaves were infiltrated with 5 μM DAF-FM DA in 0.1% dimethyl sulfoxide (DMSO) with or without 500 μM cPTIO using a 1 ml syringe without a needle. After drying for 1 h, the infiltrated plants were fumigated with NO_2. Immediately after fumigation, 6 mm leaf discs were obtained using a cork borer. The leaf discs were placed upside down into black 96-well plates containing 50 μl ddH_2O. The fluorescence of the leaf discs was measured at 485 nm excitation and 535 nm emission using a Tecan GENios microplate reader (Tecan). The average fluorescence value of leaf discs infiltrated with 0.1% DMSO (negative control) was subtracted from the sample readings. In other experiments DAF-FM DA with or without 500 μM cPTIO was co-infiltrated with 10 or 100 mM $NaNO_2$. Leaf discs were obtained 1 h after infiltration and NO content was measured as described above. NO emission from NO_2-fumigated plants was recorded using an illuminated glass chamber (0.5 l volume) connected to the room air at one side and to the CLD 88 Yp NO analyser (Eco Physics) at the other side. Plants were fumigated with NO_2, de-rooted, and placed in a dish with water that was covered by Parafilm containing holes for the cut plant hypocotyls. A total of 5 g plant material was used per treatment.

H_2O_2 generation was visualized using 3,3′-diaminobenzidine tetrahydrochloride (DAB; Sigma-Aldrich). Leaves were detached immediately after fumigation or 3 h after nitrite infiltration and vacuum-infiltrated with 1 mg ml^{-1} DAB in H_2O containing 0.05% Tween 20 (pH 3.8, KOH). After incubation for 45 min in light, the leaves were rinsed with water and transferred to 96% ethanol. The samples were incubated in a water bath at 80 °C until all chlorophyll was removed. The leaves were then rinsed three times with water and mounted in 50% glycerol for documentation. To confirm the specificity of the DAB staining to H_2O_2, plants were infiltrated with 100 U ml^{-1} CAT in 0.38 M potassium phosphate buffer pH 7. After drying for 1 h the plants were fumigated with 30 ppm NO_2 and stained as described above.

Ascorbate and glutathione measurements

After NO_2 fumigation 50 mg leaf material was sampled and homogenized in liquid N_2 as described above. Glutathione and ascorbate were extracted with 100 µl 5% metaphosphoric acid. Samples were incubated for 10 min at RT and centrifuged for 30 min at 19 000 *g*. Immediately before the measurements, samples were neutralized by adding 20 µl 1 M triethanolamine. Glutathione was determined in 50 µl and ascorbate in 20 µl neutralized extracts, as previously described (Gaupels *et al.*, 2016).

Phytohormone measurements

For quantification of phytohormones, plant material was weighed and approximately 250 mg fresh weight was harvested, immediately frozen in liquid nitrogen, and kept at –80 °C until used. The extraction procedure of the different phytohormones (jasmonic acid, JA; jasmonic acid–isoleucine conjugate, JA-Ile; *cis*-(+)-12-oxophytodienoic acid, *cis*-OPDA; salicylic acid, SA; abscisic acid, ABA) was performed as described (Vadassery *et al.*, 2012). For liquid chromatography–tandem mass spectrometry (LC-MS/MS) analyses, an Agilent 1200 HPLC system (Agilent, Waldbronn, Germany) and subsequent API 5000 tandem mass spectrometer (Applied Biosystems, Darmstadt, Germany) equipped with a Turbo spray ion source in negative ionization mode was used (Vadassery *et al.*, 2012). The elution profile was changed to 0–0.5 min, 10% B; 0.5–4.0 min, 10–90% B; 4.0–4.02 min, 90–100% B; 4.02–4.5 min, 100% B and 4.41–7.0 min, 10% B at a flow rate of 1.1 ml min^{-1}. Phytohormone amounts were calculated relative to the signal of the corresponding internal standards (Vadassery *et al.*, 2012).

Stomatal conductance measurements

Stomatal conductance to water vapor (mmol m^{-2} s^{-1}) was determined immediately after fumigation with NO, NO_2, or air using a SC-1 Leaf Porometer (Decagon Devices Inc.). To obtain a reference for the conductance of closed stomata, plants were transferred to the dark for 2.5 h before measurement to induce stomatal closure.

Statistics

Data sets passing the Shapiro–Wilk normality test (P>0.05) were analysed by one-way ANOVA and the Holm–Sidak *post hoc* test for pairwise comparisons or comparisons against a control group using SigmaPlot 12.0 (Systat Software). When the normality assumption of ANOVA failed on original or log-transformed data (Shapiro–Wilk test), the non-parametric Kruskal–Wallis test was performed to test for differences between groups using Wilcoxon tests with false discovery rate (FDR) correction for *post hoc* analysis. Non-parametric analysis was performed using R version 3.0.3. Statistical significances were indicated with asterisks (***P<0.001, **P <0.01, *P<0.05).

Results

Fumigation with NO_2 but not NO triggers cell death

Fumigation of Arabidopsis with NO_2 induced concentration-dependent leaf damage. After 1 h exposure to 30 ppm NO or 10 ppm NO_2, leaves did not show visible symptoms (Fig. 1A). NO_2 at 20 ppm caused severe lesions, while 30 ppm NO_2 caused complete leaf collapse and rapid wilting, which already started during the 1 h fumigation period (Fig. 1A). Ion leakage measurements confirmed that cell membranes were not affected by 30 ppm NO or 10 ppm NO_2 (Fig. 1B). However, relative ion leakage rose from 15% in control leaves to 30% in leaves fumigated with 20 ppm NO_2 and to 65% after treatment with 30 ppm NO_2 (Fig. 1B).

Differences in toxicity between NO and NO_2 are not dependent on stomatal conductance

Regulation of the stomatal aperture determines foliar gas uptake. Generally, stomata are open in the light for facilitating CO_2 uptake during photosynthesis but are closed in the dark in order to avoid water loss. Accordingly, measurements with a leaf porometer revealed a 50% reduction in stomatal conductance at 2.5 h after transferring plants from light into dark conditions (Fig. 2). Fumigation with either 30 ppm NO, which is not toxic to plant cells, or with 20 ppm NO_2, which induces lesion formation, triggered a significant down-regulation of stomatal conductance by approximately 20%.

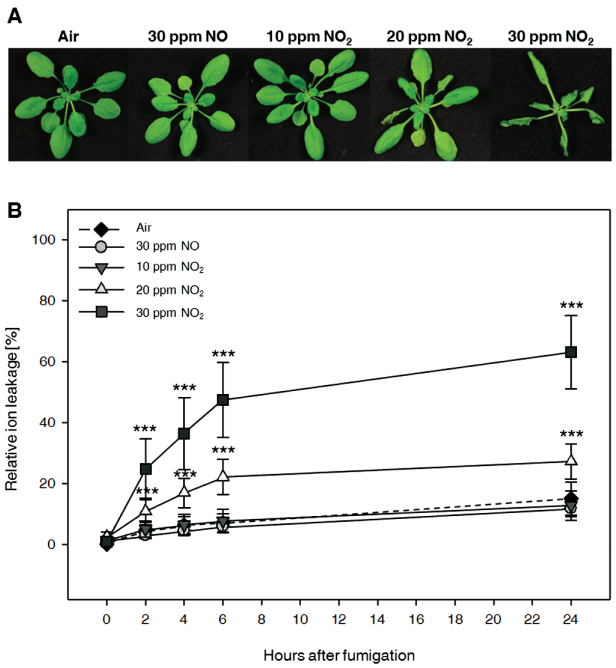

Fig. 1. NO_2 but not NO triggers cell death. Arabidopsis Col-0 plants were exposed to air (control), 30 ppm NO or 10, 20, and 30 ppm NO_2 for 1 h. (A) Representative visible symptoms at 24 h after fumigation. (B) Cell death was assayed by electrolyte leakage measurements at various time points after treatment. Data points are means (±SD, n=10–19). Asterisks indicate significant differences from control samples (Kruskal–Wallis test and Wilcoxon test with FDR correction, ***P<0.001). (This figure is available in color at *JXB* online.)

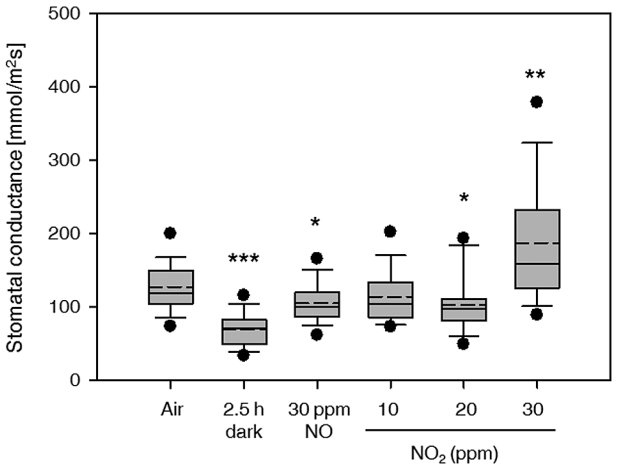

Fig. 2. NO_2 and NO influence stomatal conductance. Directly after fumigation with NO or NO_2 for 1 h stomatal conductance was measured using a leaf porometer. As a reference for stomatal closure plants were transferred to the dark for 2.5 h. Box plots represent median (solid line), mean (dotted line) and 25th/75th percentiles (grey box); whiskers represent 5th and 95th percentiles; black dots are outliers (n=14–40). Asterisks indicate significant differences from control samples (Kruskal–Wallis test and Wilcoxon test with FDR correction, *P<0.05, **P<0.01, ***P<0.001).

These results suggest that the stomatal uptake of 30 ppm NO and 20 ppm NO_2 is similar and does not correlate with the different toxicities of the gases. NO_2 at 30 ppm caused a 75% increase in stomatal conductance that could be mechanistically linked to the rapid wilting symptoms.

NO_2 fumigation causes an increase in nitrogen compounds and peptide modifications by reactive nitrogen species

NO_2 and NO have a different chemistry in aqueous solutions. NO_2 disproportionates into equimolar amounts of nitrite and nitrate, whereas NO decays to nitrite (Ignarro *et al.*, 1993). Nucleophilic molecules including proteins and peptides are nitrated by NO_2 but *S*-nitrosylated by NO (Gaupels *et al.*, 2011).

Basal nitrite concentrations of approximately 1 nmol mg^{-1} protein in control leaves gradually increased to 3500 nmol mg^{-1} protein after fumigation with 30 ppm NO_2 while at the same time SNO levels multiplied by a factor of 12, from 49 to 610 pmol mg^{-1} protein (Fig. 3A, B). However, 30 ppm NO had no effect on nitrite levels, and only one of three independent experiments showed a measurable increase in SNO levels. NR has a high turnover rate, keeping nitrate concentrations rather stable. Only 30 but not 10 or 20 ppm NO_2 resulted in an, insignificant, increase of the nitrate content. Nitrate was significantly reduced from 26 µmol mg^{-1} protein in control samples to 9 µmol mg^{-1} protein after fumigation with 30 ppm NO (Fig. 3C). Nitration of tyrosine residues upon NO_2 fumigation occurred in a different pattern than *S*-nitrosylation. NO_2 at 10 and 20 ppm caused a 1.5- and 2.8-fold accumulation, but 30 ppm NO_2 showed a 57-fold accumulation, of nitrotyrosine-containing proteins compared with control (Fig. 3D). Tyrosine nitration was not influenced by NO. In summary, NO_2 fumigation loads the leaf with nitrite and SNOs, but pronounced tyrosine nitration occurred only with 30 ppm NO_2.

H_2O_2, NO, and antioxidants are involved in NO_2-induced cell death

NO and H_2O_2 are essential signals for the initiation of HR (Leitner *et al.*, 2009). For this reason, the intracellular NO formation was investigated by the fluorescent dye diaminoflouresceine diacetate (DAF-FM DA). NO_2 caused a non-significant induction of DAF-FM DA fluorescence at 20 ppm but a statistically significant 2.2-fold induction at the 30 ppm concentration (Fig. 4A). DAF fluorescence was reduced in the presence of the NO scavenger cPTIO. NO emission from NO_2 fumigated leaves was determined by using a NO analyser. NO emission was low to moderate after 10 and 20 ppm NO_2 but was high after 30 ppm NO_2 indicating a non-linear relationship between NO_2 concentration and NO emission from leaves (Fig. 4B). Emission of NO_2 was not detected (not shown), suggesting that all NO_2 loaded into or produced within the leaves was bound or degraded. It is noteworthy that DAF-FM DA was probably not sensitive enough for monitoring the low intracellular NO accumulation after fumigation with 10 and 20 ppm NO_2.

H_2O_2 accumulation was detected by DAB staining after fumigation with 20 and 30 but not 10 ppm NO_2 (Fig. 4C). Hence, the rise in H_2O_2 correlated with cell death symptoms induced by 20 and 30 ppm NO_2. Injection of the H_2O_2-detoxifying enzyme catalase prior to fumigation with 30 ppm NO_2 largely prevented the DAB staining. A further indication of redox signaling upon NO_2 fumigation was provided by photometric measurements of the major antioxidants ascorbate and glutathione. Reduced glutathione (GSH) and reduced ascorbic acid (AsA) were both depleted after fumigation with 30 ppm NO_2 by approximately 90 and 80%, respectively. Oxidized glutathione (GSSG), however, was 5-fold up-regulated, whereas dehydroascorbate (DHA) levels were not changed significantly (Fig. 4D).

A role of NO and H_2O_2 as death signals was substantiated by pre-injection of leaves with cPTIO and catalase before fumigation. Both reduced NO_2-induced ion leakage by about 40% compared with control injections (Fig. 5). Moreover, pre-treatment of plants with 30 ppm NO or 10 ppm NO_2 4 h prior to a secondary fumigation with 30 ppm NO_2 caused a 40% higher ion leakage as compared with 30 ppm NO_2 alone (see Supplementary Fig. S1), supporting a death-promoting role of NO and NO_2.

In summary, a rapid accumulation of NO and H_2O_2 as well as depletion of antioxidants caused by NO_2 fumigation was observed simultaneous to apparent leaf damage. NO scavenging and H_2O_2 degradation partially prevented NO_2-induced cell death.

Salicylic acid, jasmonates, and abscisic acid signaling are induced during NO_2-induced cell death

The phytohormones SA, jasmonates, and abscisic acid (ABA) are well-known players in plant defense responses

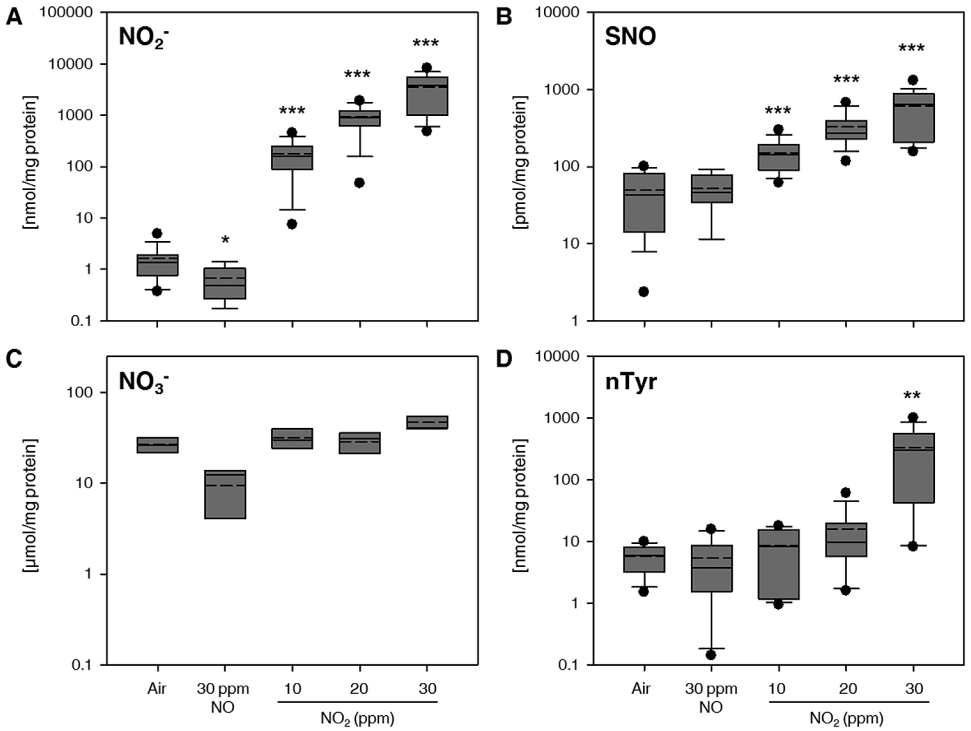

Fig. 3. Nitrite, nitrate, *S*-nitrosothiols, and nitrated proteins accumulate upon NO_2 fumigation. Arabidopsis plants were exposed to air (control) or NO_2 for 1 h. (A–C) Nitrite (NO_2^-) (A), *S*-nitrosothiols (SNO) (B) and nitrate (NO_3^-) (C) were measured by a nitric oxide analyser; (D) a commercial enzyme-linked immunoassay was used for quantification of tyrosine-nitrated proteins (nTyr). Box plots represent median (solid line), mean (dotted line) and 25th/75th percentiles (grey box); whiskers represent 5th and 95th percentiles (only when $n>3$); black dots are outliers (n=9–14 (A), 8–14 (B), 3 (C), 8–11(D)). Asterisks indicate significant differences from control samples (Kruskal–Wallis test and Wilcoxon test with FDR correction, *$P<0.05$, **$P<0.01$, ***$P<0.001$).

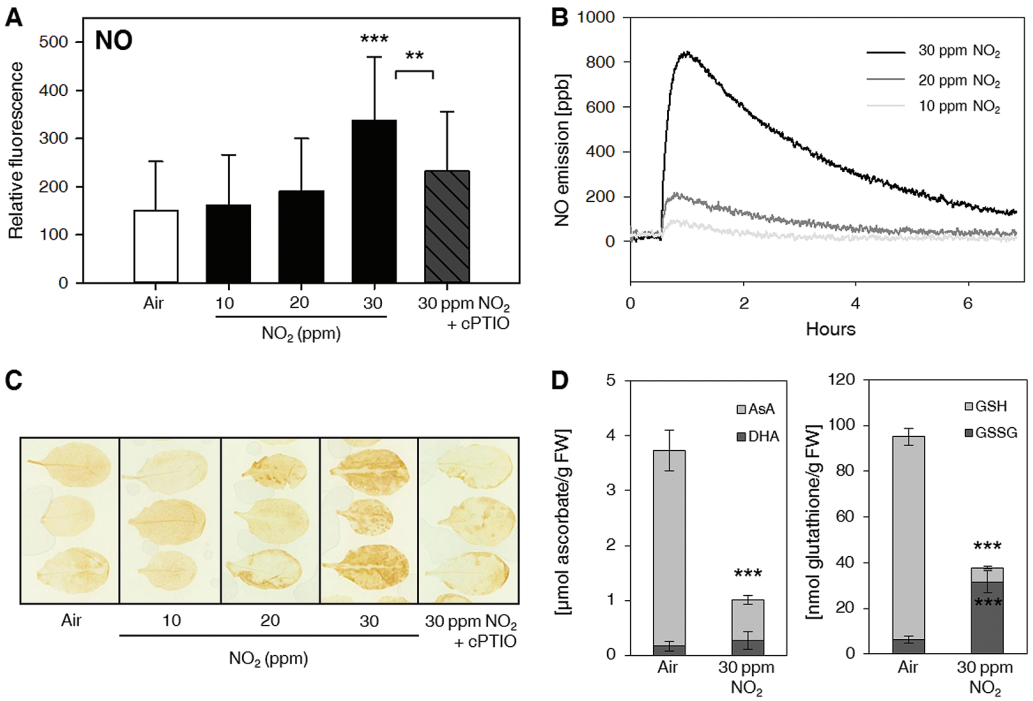

Fig. 4. NO_2 fumigation triggers NO and H_2O_2 signaling and a decrease in antioxidants. Arabidopsis plants were exposed to air (control) or NO_2 for 1 h. (A) Intracellular NO was quantified using a photometric assay based on 4,5-diaminofluorescein-FM diacetate (DAF-FM DA). Injection of the NO scavenger cPTIO (500 µM) before fumigation with 30 ppm NO_2 served as a negative control for the DAF-FM DA staining. (B) NO emission from plants fumigated with NO_2 was measured by a nitric oxide analyser. (C) H_2O_2 detection by 3,3′-diaminobenzidine (DAB). Injection of the H_2O_2-degrading enzyme catalase (CAT, 100 U ml^{-1}) before fumigation with 30 ppm NO_2 served as negative control for the DAB staining. (D) Levels of reduced ascorbate (ASA), dehydroascorbate (DHA), reduced glutathione (GSH), and oxidized glutathione (GSSG) were determined by photometric assays. Columns represent means (±SD, n=23–24 (A), 5–9 (C) 5 (D)). Asterisks indicate significant differences from control samples (one-way ANOVA with Holm–Sidak *post hoc* test for multiple comparisons *versus* control group, **$P<0.01$, ***$P<0.001$). (This figure is available in color at *JXB* online.)

(Pieterse *et al.*, 2012). NO_2 at 30 ppm triggered a 6.5-fold increase in SA levels immediately after fumigation (0 h time point). Concentrations peaked at almost 2000 ng g^{-1} FW at 3 and 6 h after the treatment followed by a decline at 24 h (Fig. 6). JA showed similar kinetics with a more pronounced 21-fold accumulation directly after NO_2 exposure and maximum concentrations of 4100 ng g^{-1} FW at the 6 h time point. The bioactive JA derivative JA-Ile was increased by a factor of 24 directly after NO_2 exposure culminating in peak levels around 200 ng g^{-1} FW at the 6 and 24 h time points. The measured 2- to 6.5-fold accumulation of the JA precursor *cis*-OPDA was rather moderate compared with the other jasmonates. ABA levels were not altered significantly immediately after fumigation, but increased up to 8-fold at 24 h reaching concentrations of 41 ng g^{-1} FW. Thus, SA, JA, and JA-Ile were strikingly induced by NO_2 and might act as early cell death signals. ABA may be implicated in signaling events later than the investigated 24 h time point.

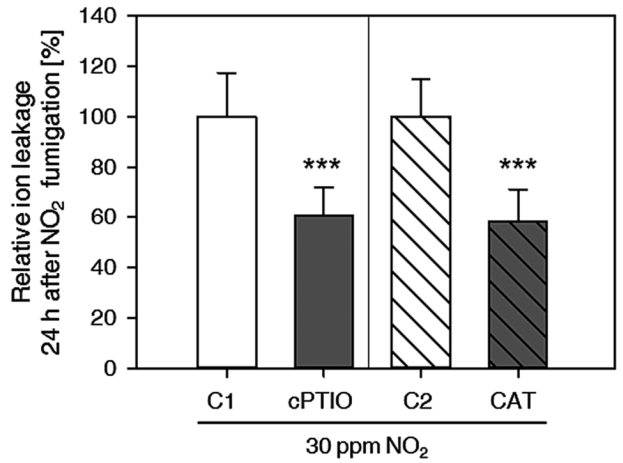

Fig. 5. Scavengers of NO and H_2O_2 prevent NO_2-induced cell death. Leaves were injected with water (control 1, C1), 500 µM cPTIO, phosphate buffer (control 2, C2) or 100 U ml^{-1} catalase (CAT) 1 h before exposure to 30 ppm NO_2. Plants were harvested directly after fumigation and ion leakage was measured 24 h later. Columns represent means (±SD, *n*=5). Asterisks indicate significant differences from control samples (one-way ANOVA with Holm–Sidak *post hoc* test for multiple comparisons *versus* control group, ***P<0.001).

Mutants related to stress and defense signaling are altered in NO_2 sensitivity

Cell death induced by 1 h fumigation with 30 ppm NO_2 was evaluated for mutants and transgenic plants with disturbed NO, ROS, JA, SA, ethylene, and ABA signaling. Besides ion leakage, basal stomatal conductance was determined to assess the contribution of altered NO_2 uptake to the observed mutant phenotypes. This approach was aimed at identifying further players involved in the NO_2 response.

Mutants affected in NO and ROS homeostasis exhibited the highest sensitivity towards NO_2 (Table 2). The *nia1nia2noa1* triple mutant is devoid of NR (*nia1nia2*) and NITRIC OXIDE ASSOCIATED1 (*noa1*)—a cGTPase indirectly involved in NO production (Moreau *et al.*, 2008). This perturbation in nitrogen metabolism caused a 31.9% increase in ion leakage compared with wild-type (WT). The NO and arginine over-accumulating *nox1* mutant had WT stomatal conductance but ion leakage was 36.9% higher than in WT plants. The enzyme GSNO reductase (GSNOR) is involved in NO homeostasis. *GSNOR* knock-out (*gsnor*) and antisense (*GSNOR-AS*) plants were more sensitive to 30 ppm NO_2 than WT plants, but only *gsnor* displayed an elevated stomatal conductance. The NADPH oxidase mutant *rbohF* had an enhanced stomatal conductance accompanied with a rather moderate NO_2 sensitivity. However, *rbohD* plants exhibited 26.2% more cell death than WT, without a significant increase in stomatal opening. *vtc1* and *gsh1* have reduced levels of ascorbate and glutathione, which caused an enhanced sensitivity, indicating that antioxidants protect plants from NO_2

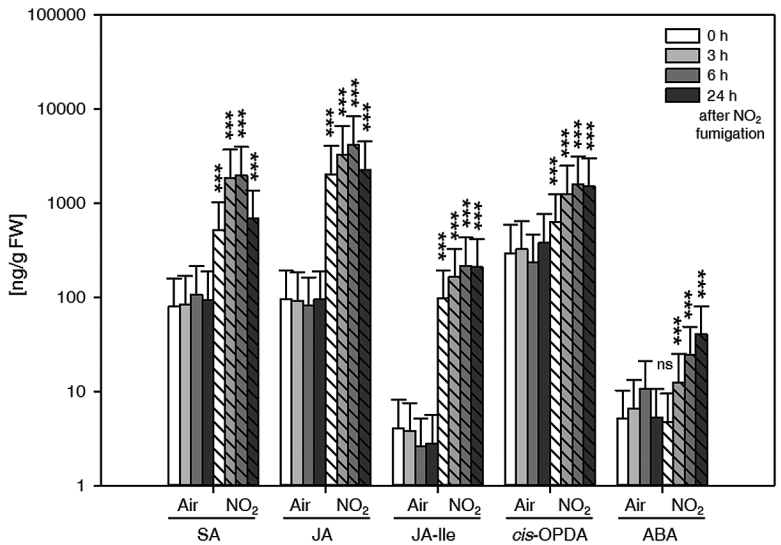

Fig. 6. NO_2-induced alteration of phytohormone levels. Arabidopsis plants were fumigated with 30 ppm NO_2 for 1 h and leaves were collected directly (0 h), 3, 6, and 24 h after the 1 h fumigation period. Salicylic acid (SA), jasmonic acid (JA), JA-isoleucine (JA-Ile), *cis*-(+)-12-oxophosphodienoic acid (*cis*-OPDA), and abscisic acid (ABA) were measured by LC-MS/MS. Columns represent means (±SD, *n*=5). Asterisks indicate significant differences from respective control samples (one-way ANOVA with Holm–Sidak *post hoc* test for all pairwise comparisons; ns: not significant; ***P<0.001).

Table 2. *NO_2 phenotypes of NO, ROS and phytohormone mutants*

Median change compared with wild-type (%) (95% confidence interval). *n*=6–9 for ion leakage; *n*=12–22 for stomatal conductance. Level of statistical significance (Kruskal–Wallis test with Wilcoxon rank sum *post hoc* test): ***P* adj<0.001; **P* adj<0.01; *P* adj<0.05; n.s., not significant.

Genotype	Ion leakage	Stomatal conductance
Nitric oxide		
nia1nia2noa1	31.9 (21.9, 41.2)***	–10.0 (–19.5, 0.3) n.s.
nox1	36.9 (27.2, 42.5)***	2.0 (–13.7, 17.8) n.s.
gsnor	27.4 (18.8, 40.5)***	24.2 (12.5, 36.0)***
GSNOR-AS	21.7 (11.4, 32.2)***	–9.0 (–21.8, 0.0) n.s.
Reactive oxygen species		
rbohD	26.2 (18.3, 31.3)***	10.0 (–1.3, 21.9) n.s.
rbohF	20.6 (12.9, 28.8)***	18.0 (6.8, 28.9)**
gsh1	14.2 (5.4, 25.1)**	–19.8 (–28.4, –10.1)***
vtc1	14.6 (8.9, 20.4)***	–1.9 (–10.1, 8.3) n.s.
Jasmonic acid		
aos	4.4 (–0.8, 11.9) n.s.	3.9 (–4.5, 12.6) n.s.
coi1	5.5 (–0.5, 10.8) n.s.	3.1 (–7.3, 15.3) n.s.
jar1	9.8 (4.2, 15.9)*	2.1 (–5.0, 9.3) n.s.
Salicylic acid		
sid2	11.5 (3.9, 16.2)**	0.9 (–8.5, 13.3) n.s.
NahG	14.5 (6.7, 21.0)**	2.2 (–9.9, 12.0) n.s.
npr1	18.4 (12.7, 25.6)***	–1.1 (–9.4, 7.9) n.s.
Ethylene		
ein2	–6.2 (–17.8, 6.7) n.s.	–8.0 (–21.0, 3.1) n.s.
eto1	27.8 (21.1, 34.7)***	32.1 (18.3, 42.9)***
etr1	20.8 (15.5, 26.2)***	–1.5 (–11.6, 13.4) n.s.
Abscisic acid		
aba2	26.6 (19.6, 32.5)***	129.6 (112.9, 145.9)***
aba3	15.5 (8.2, 21.6)***	65.9 (36.9, 96.0)***
abi4	13.7 (6.4, 18.1)***	59.8 (45.9, 69.9)***

damage (Table 2). Both mutants had unchanged or decreased stomatal conductance.

The JA deficient mutant *aos* and the JA signaling mutant *coi1* displayed no NO_2 phenotype. These results imply that a functional JA signaling pathway is not crucial for cell death induction by NO_2. However, *jar1*, which is defective in JA-Ile synthesis, was sensitive to NO_2. Mutations in these JA mutants did not affect stomatal conductance. SA deficient *sid2* and NahG plants as well as the SA signaling mutant *npr1* were moderately sensitive to NO_2 (11.5–18.4% higher ion leakage than WT), which was independent of stomatal closure. NO_2 phenotypes of ethylene and ABA mutants largely correlated with altered stomatal conductance (Table 2). Ion leakage as well as stomatal conductance of the ethylene insensitive mutant *ein2* was similar to WT, whereas both parameters were increased in the ethylene over-accumulating mutant *eto1*. Only the ethylene resistant mutant *etr1* showed a 20.8% higher NO_2 sensitivity compared with WT without altered stomatal conductivity. *aba2* is fully ABA deficient, which accounted for a rise in stomatal conductance by 129.6% and in ion leakage by 26.6% compared with WT. The ABA mutants *aba2*, *aba3*, and *abi4* showed the most dramatic stomata phenotypes while the increases in NO_2 sensitivity were rather moderate compared with other mutants tested.

Collectively, the presented data suggest that NO and ROS are major players in NO_2-induced cell death whereas SA and ABA rather function as modulators.

Nitrite is the driver of NO_2-induced S-nitrosothiol formation, H_2O_2 signaling, and cell death

Loading leaves with NO_2 caused a massive accumulation of nitrite (Fig. 3A). Therefore, we investigated whether nitrite injection could mimic the effects of NO_2 fumigation including cell death induction. Treatment with 10 mM nitrite caused a 4.6-fold increase in nitrite and a 3-fold increase in SNO concentrations. However, these metabolites were 1283- and 51-fold increased after infiltration of 100 mM nitrite (Fig. 7A and B). Absolute levels of nitrite and SNO were similar after fumigation with 10 ppm NO_2 and injection with 10 mM nitrite. Nitrite at 100 mM caused a 3.7- to 4-fold higher accumulation than 30 ppm NO_2. Nitrotyrosine modifications were not strongly affected by nitrite (Fig. 7E) but nitrate was 1.6-fold up-regulated by 100 mM nitrite (Fig. 7D). NO formation was 4.7- to 7-fold induced by 10 and 100 mM nitrite injection, suggesting that nitrite is a more efficient NO precursor than NO_2 (Fig. 7C). Nitrite at 100 but not 10 mM triggered detectable H_2O_2 production (Fig. 7F) and cell death (Fig. 8).

Discussion

Short-term fumigation of plants with high NO_2 concentrations in the parts per million range results in growth retardation and necrotic lesions (Taylor and Eaton, 1966; Zeevaart, 1976; Liu *et al.*, 2015). The degree of NO_2 sensitivity was found to vary between different plant species. For instance, 30% of the leaf area of *Pisum sativum* (pea) was damaged after exposure to 10 ppm NO_2 for 1 h and *Solanum tuberosum* showed 55% injury after 1 h fumigation with 13 ppm NO_2 (Zeevaart, 1976). *Nicotiana glutinosa* proved to be particularly sensitive with necrotic lesions covering 70% of the leaf surface upon treatment for 1 h with 5 ppm NO_2. On the other hand, 11 ppm NO_2 for 3 h did not cause any visible symptoms to the closely related species *Nicotiana rustica* (Zeevaart, 1976).

In this work, an experimental system was established for investigating the response of Arabidopsis to acute NO_2 exposure. During the 1 h fumigation period *Arabidopsis thaliana* ecotype Col-0 plants were illuminated and NO_2 and NO concentrations were constantly monitored. The focus was directed towards early NO_2-triggered events. Therefore, samples were collected immediately after fumigation. Under these controlled conditions 10, 20, and 30 ppm NO_2 had distinct effects on Arabidopsis (Fig. 1). NO_2 at 10 ppm did not have any visible impact on the plants. However, 20 ppm NO_2 evoked severe lesions and 30 ppm NO_2 caused complete leaf collapse and wilting. These results are in accordance with a recent report showing that exposure of Arabidopsis to

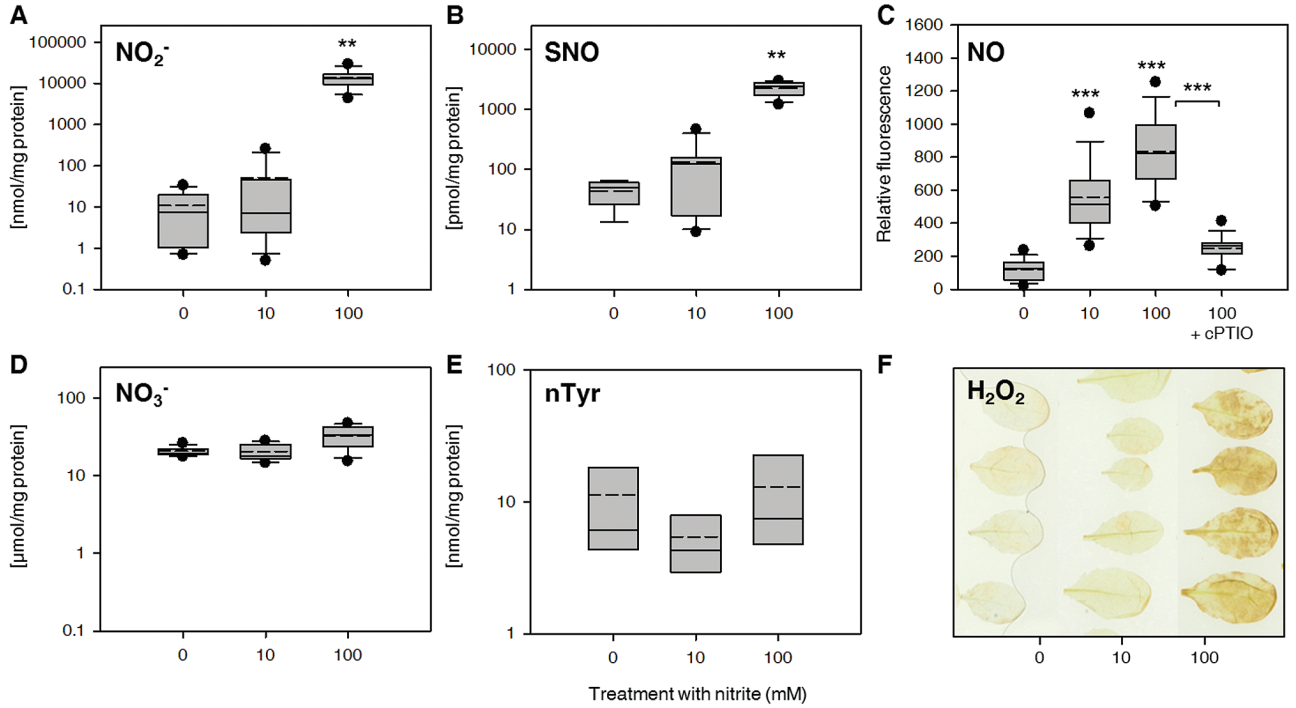

Fig. 7. Nitrite injection mimics effects of NO_2 fumigation. Leaves were injected with water (control) or nitrite. Measurements were performed 3 h after injection. (A,B,D) A nitric oxide analyser was used to determine the concentrations of nitrite (NO_2^-; A), *S*-nitrosothiols (SNO; B) and nitrate (NO_3^-; D). (E) Tyrosine-nitrated proteins (nTyr) were measured by an enzyme-linked immunoassay. (C) Intracellular NO was measured with a 4,5-diaminofluoresceine-FM diacetate-based assay and injection of cPTIO (500 µM) served as negative control. (F) H_2O_2 was detected by 3,3′-diaminobenzidine staining. Box plots represent median (solid line), mean (dotted line) and 25th/75th percentiles (grey box); whiskers represent 5th and 95th percentiles (only when $n>3$); black dots are outliers ($n=7$ (A), 4–7 (B), 10 (C), 7 (D), 3–4 (E), 8–11 (F)). Asterisks indicate significant differences from control samples (Kruskal–Wallis test and Wilcoxon test with FDR correction, $^{**}P<0.01$, $^{***}P<0.001$). (This figure is available in color at *JXB* online.)

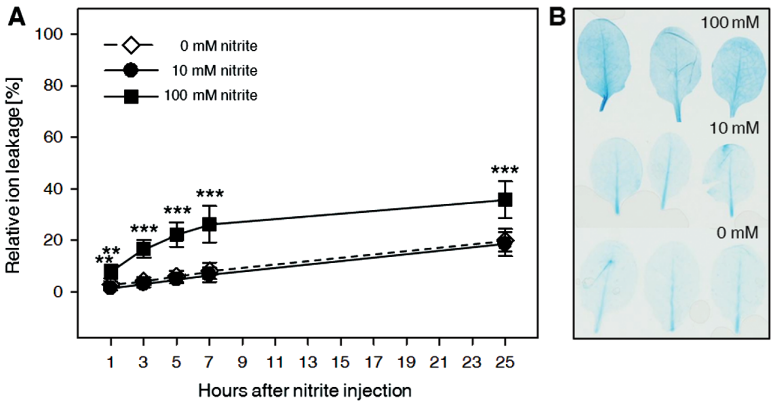

Fig. 8. Nitrite triggers cell death. Four leaves per plant were injected with water (control), 10 mM nitrite or 100 mM nitrite. (A) Cell death was quantified by electrolyte leakage measurements of whole rosettes starting 1 h after injection. Data points are means (±SD, $n=15$–16). Asterisks indicate significant differences from control samples (Kruskal–Wallis test and Wilcoxon test with FDR correction, $^{**}P<0.01$, $^{***}P<0.001$). (B) Trypan blue staining of dead cells at 24 h after nitrite injection. (This figure is available in color at *JXB* online.)

9.2 ppm (18.8 mg m^{-3}) NO_2 for 6 h per day led to death of the entire plants within 1 week of repeated treatments.

The observed rapid lesion formation after 30 ppm NO_2 resembled the symptoms after infection with avirulent pathogens or acute ozone treatments. For instance, infection of Arabidopsis with a high load of avirulent *Pseudomonas syringae* leads to HR and ultimately programmed cell death within 4 h (Katagiri *et al.*, 2002). Exposure for 3 h to 300 ppb (parts per billion) ozone triggered necrotic lesions in the sensitive Arabidopsis accession Cvi-0 (Rao and Davis, 1999). Pathogen- and ozone-triggered cell death events are well characterized and will therefore be compared with NO_2-induced cell death throughout the discussion. Contrary to 20 and 30 ppm NO_2, Arabidopsis leaves were not damaged by 30 ppm NO. Even fumigation with 60 ppm NO for 12 h was not toxic (Frungillo *et al.*, 2014). NO is known to be involved in stomatal closure (Desikan *et al.*, 2002), which could prevent leaf uptake of the gas. However, leaf damage did not correlate with stomatal conductance, since 30 ppm NO and 20 ppm NO_2 both triggered partial stomatal closure (Fig. 2) while only the latter caused severe symptoms.

Alternatively, the different toxicities of NO_2 and NO might be based on their distinct molecular properties. In the leaf NO_2 disproportionates to equal amounts of nitrite and nitrate. Nitrate reductase (NR) converts nitrate into nitrite, which is further processed to ammonium by nitrite reductase (NiR; Crawford, 1995). The massive accumulation of nitrite hints at NiR being the rate limiting enzyme in NO_2 metabolization (Zeevaart, 1976). This corresponds to the observation that NO_2 acted as an efficient nitrite donor whereas the nitrate level was not significantly changed (Fig. 3A, C). Similar results were previously found for pea (Zeevaart, 1976). Conversely, NO fumigation resulted in lowered levels of these N compounds, either through stimulation of NiR and NR activities or via the inhibition of cellular uptake mechanisms of nitrate and nitrite. Previously, it was found that NO donors enhanced the NR activity and consequently decreased the nitrate concentration in leaves and roots of *Brassica chinensis* (Du *et al.*, 2008). Contrariwise, the reduced nitrate content in the Arabidopsis NO accumulating mutant *nox1* was based on down-regulated nitrate uptake by specific transporters (Frungillo *et al.*, 2014).

Loading leaves with NO_2 induced protein modifications by *S*-nitrosylation and tyrosine nitration. *S*-nitrosylation arises from the binding of NO to sulfhydryl groups (–NO adduct), whereas nitration of tyrosine residues (–NO_2 adduct) is mediated by peroxynitrite, which is the reaction product of NO and superoxide (Gaupels *et al.*, 2011; Kovacs and Lindermayr, 2013; Yu *et al.*, 2014). Both modifications are NO dependent; therefore it was unexpected that 30 ppm NO did not provoke a significant rise in *S*-nitrosylated and nitrated proteins. Other researchers exposed Arabidopsis plants to 60 ppm NO for 12 h, which resulted in a moderate buildup of *S*-nitrosothiols (SNOs; Frungillo *et al.*, 2014). In comparison, SNO formation already occurred after fumigation with 10 pm NO_2 and tyrosine nitration was detected after treatment with 30 ppm NO_2 for 1 h (Fig. 3B, D). Hence, NO_2 is a more efficient donor for NO-dependent protein modifications than NO itself.

Different techniques were used for a more detailed investigation of NO signaling during plant responses to NO_2. Photometric measurements with the fluorescent probe DAF-FM DA demonstrated a weak increase in intracellular NO after exposure to 30 ppm NO_2 (Fig. 4A). On the other hand, all tested doses of NO_2 caused significant NO emission from the leaves (Fig. 4B). The particular strong NO release induced by 30 ppm NO_2 was likely facilitated by the increased stomatal conductance after this treatment. Collectively, the presented results imply that NO_2 is reduced to nitrite and NO in the acidic conditions of the apoplast. NO is released from the leaves through the stomata while a proportion also enters the cell as evidenced by the increased DAF staining and *S*-nitrosylation. Endogenous NO production by NR (NIA1/NIA2) and a NOA1-dependent enzyme activity are not important for the onset of NO_2-induced cell death since the *nia1nia2noa1* triple mutant did not display less but even more NO_2-induced cell death compared with WT.

NO signaling during cell death has been reported frequently. Amongst others, experiments with soybean cell cultures, Arabidopsis, and tobacco have consistently shown synthesis of NO and subsequent protein *S*-nitrosylation as well as tyrosine nitration after inoculation with different avirulent pathovars of *Pseudomonas syringae* (Delledonne *et al.*, 1998; Romero-Puertas *et al.*, 2008; Cecconi *et al.*, 2009; Scheler *et al.*, 2013; Wang *et al.*, 2013). Similarly, leaf damage after exposure of Arabidopsis and poplar (*Populus* × *canescens*) to ozone was accompanied by NO signaling and changes in the *S*-nitrosoproteome (Ahlfors *et al.*, 2009; Vanzo *et al.*, 2016).

Like NO, H_2O_2 is regarded as a general stress messenger and was demonstrated to function as a death signal during HR (Levine *et al.*, 1994). DAB staining revealed the production of H_2O_2 after 20 and 30 ppm NO_2, which correlated with the occurrence of leaf symptoms (Fig. 4C). The NADPH oxidases RBOHD and F are major ROS-generating enzymes during plant defense responses including HR and ozone-induced cell death (Torres and Dangl, 2005; Gilroy *et al.*, 2014; Mignolet-Spruyt *et al.*, 2016). However, *rbohD* and *rbohF* mutants were not compromised in NO_2-induced cell death, suggesting that apoplastic peroxidases and other sources might contribute to the ROS burst.

Meanwhile, it is widely accepted that only the cooperative action of both redox signals H_2O_2 and NO efficiently triggers cell death (Leitner *et al.*, 2009; Scheler *et al.*, 2013; Wang *et al.*, 2013). Low micromolar concentrations of H_2O_2 were sufficient for the induction of cell death if soybean (*Glycine max*) cell cultures were co-treated with the NO donor sodium nitroprusside (SNP; Delledonne *et al.*, 1998). Conversely, SNP was only an effective death stimulus if co-treated with H_2O_2. After infection with an avirulent strain of *Pseudomonas syringae*, soybean cells displayed more HR when SNP was added to the culture medium. Likewise, the pathogen-elicited HR was diminished by an inhibitor of RBOH activity, catalase-mediated scavenging of H_2O_2 or cPTIO-mediated scavenging of NO (Delledonne *et al.*, 1998).

Accordingly, leaf injection of cPTIO or CAT prior to NO_2 fumigation reduced the ion leakage by approximately 40%, when compared with control-injected leaves (Fig. 5). This demonstrated that NO_2-induced cell death was largely dependent on NO and H_2O_2. The important function of redox signaling during NO_2-induced cell death was further substantiated by mutant analyses. The NO accumulating mutants *nox1*, *gsnor* and *GSNOR-AS* as well as the antioxidant-deficient mutants *gsh1* and *vtc1* were all NO_2 sensitive. Current models consider NO as an amplifier of H_2O_2 signaling by inhibiting enzymes of the antioxidant system (Groß *et al.*, 2013; Begara-Morales *et al.*, 2016). In such a scenario, the decrease in glutathione and ascorbate levels after fumigation with 30 ppm NO_2 (Fig. 4D) could be considered to be a mechanism for the amplification of ROS signaling. This is consistent with the finding that H_2O_2 and NO treatment of tobacco BY-2 cells caused cell death accompanied by a depletion of the antioxidants (de Pinto *et al.*, 2002).

NO_2 is not stable in the aqueous environment of leaf tissues. Therefore, it was assumed that NO_2-induced effects were actually mediated by nitrite, which strongly accumulates after fumigation with all NO_2 concentrations used. This hypothesis was tested by nitrite injections into leaves. Nitrite at 100 mM

had a similar impact on the leaf physiology as 30 ppm NO_2 including cell death induction and the accumulation of nitrite, SNO, NO and H_2O_2 (Fig. 8). However, nitrite treatment did not result in tyrosine nitration although NO and ROS were both detected. Most likely, the strong increase in NO content and the resultant high NO:ROS ratio after nitrite injection favors formation of the *S*-nitrosylating N_2O_3 whereas accumulation of the nitrating $ONOO^-$ requires a high ROS:NO ratio (Thomas *et al.*, 2008). By contrast, 10 mM nitrite caused a significant increase in NO, but SNO and H_2O_2 did not accumulate and cell death was not increased, suggesting that both H_2O_2 and NO are necessary for nitrite-induced cell death.

NO_2-induced cell death was accompanied by a massive increase in the concentrations of SA, JA, JA-Ile, *cis*-OPDA, and ABA. Interactions of these phytohormones in plant cell death events are complex and still not fully resolved. High SA levels in cells infected by an avirulent pathogen promote death, whereas intermediate levels in nearby uninfected cells favor cell survival in order to prevent uncontrolled spreading of lesions (Yan and Dong, 2014). Such a dose-dependent effect of SA on cell death was also seen after exposure of Arabidopsis to ozone and NO_2. High ozone-induced SA levels in the sensitive accession Cvi-0 facilitated cell death, whereas the moderate SA content in Col-0 diminished leaf damage by activating the antioxidant machinery (Rao and Davis, 1999; Rao *et al.*, 2000). After fumigation with 30 ppm NO_2, the SA biosynthesis mutant *sid2* and transgenic plants expressing the bacterial SA hydrolase NahG and the *npr1* signaling mutant all displayed moderate NO_2 sensitivity. These results argue for a protective function of basal SA against NO_2 damage. Nevertheless, the lesion formation in SA mutants highlights that a functional SA signaling pathway is not a prerequisite for NO_2-induced cell death.

Jasmonates and other oxidized lipids regulate detoxification and stress responses (Müller *et al.*, 2008; Farmer and Müller, 2013). For instance, JA regulates genes related to the antioxidant system and secondary metabolism (Sasaki-Sekimoto *et al.*, 2005; Taki *et al.*, 2005). Gene regulation by JA and the bioactive conjugate JA-Ile is controlled by the receptor component CORONATINE INSENSITIVE1 (COI1; Browse, 2009) whereas the *cis*-OPDA-mediated induction of genes related to cell protection and survival is independent of COI1 (Taki *et al.*, 2005). Consistent with these findings, several JA biosynthesis and signaling mutants were more sensitive to ozone than WT plants (Overmyer *et al.*, 2000; Rao *et al.*, 2000). Pre-treatment of plants with methyl-JA before exposure to ozone prevented the development of symptoms (Rao *et al.*, 2000). However, only *jar1* showed a weak sensitivity phenotype in response to NO_2 fumigation and independent of stomatal conductance. The *coi1* signaling mutant and the *aos* mutant, which is defective in JA production, were both not significantly altered in their NO_2 response. This argues against a major role of JA signaling in the protection from NO_2 damage. The distinct increases in jasmonates after NO_2 exposure might influence stress responses other than cell death induction including defense gene expression.

The simultaneous accumulation of SA and JA has been reported after acute ozone exposure (Rao *et al.*, 2000), as well as the onset of HR (Kourtchenko *et al.*, 2007), and could be part of a general plant response triggered by strong stress stimuli. In such a situation JA signaling is overruled by SA (Pieterse *et al.*, 2012). After the death-promoting stress-induced SA peak the JA signaling pathway would be derepressed and cell survival mechanisms would be activated to avoid excessive tissue damage.

The NO_2 responses of ethylene and ABA mutants were mainly dependent on the stomatal conductance. Only the ethylene receptor mutant *etr1* showed more necrotic lesions than WT plants without altered stomatal regulation. However, two other ethylene mutants tested did not show distinct phenotypes and the NO_2 sensitivity of *etr1* could be caused by the increased levels of ABA, cytokinin, auxin, and gibberellin as previously reported for this mutant (Chiwocha *et al.*, 2005). In this regard it is interesting that a *coi1 ein2 sid2* triple mutant defective in JA, SA, and ethylene signaling displayed lesions after ozone exposure, implying that these hormones are not essential for cell death induction (Xu *et al.*, 2015). Mutants compromised in ABA biosynthesis (*aba2*, *aba3*), and signaling (*abi4*) were less sensitive than expected, since their high stomatal conductance is indicative of a facilitated NO_2 uptake. This would point to a damage-promoting role of ABA. The late peak of ABA at 24 h after NO_2 fumigation hints at a function of this hormone in late stress/cell death signaling.

In summary, NO_2-triggered cell death was dependent on NO and H_2O_2 and was accompanied by protein *S*-nitrosylation, tyrosine nitration and the depletion of antioxidants (Fig. 9). SA, jasmonates, and ABA strongly accumulated after fumigation with 30 ppm NO_2, but mutant analyses demonstrated that these defense hormones were not essential for cell death induction. The features of NO_2-induced cell death resemble PCD in response to ozone or infection by avirulent pathogens. However, necrotic lesions appeared already within 1 h of NO_2 fumigation whereas PCD-related symptoms are

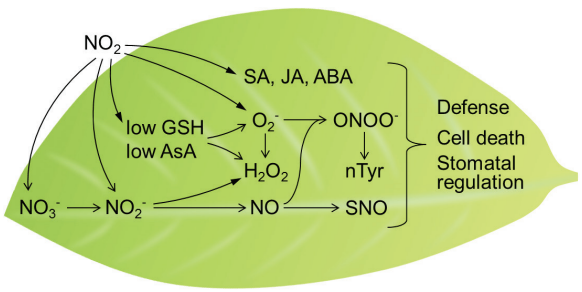

Fig. 9. Summary of NO_2 effects. Fumigation with NO_2 caused the accumulation of nitrate (NO_3^-) and nitrite (NO_2^-). Nitrite was probably converted to NO, which binds to peptides thereby forming *S*-nitrosothiols (SNO). Nitrite also triggered H_2O_2 production. NO and H_2O_2 are well-known inducers of defense responses, cell death and stomatal closure. NO_2 but not nitrite induced protein tyrosine nitration (nTyr), which is an indirect indicator for the simultaneous formation of superoxide (O_2^-) and peroxynitrite ($ONOO^-$). NO_2 induced a drop in glutathione (GSH) and ascorbate (AsA) and a massive increase in the defense-related phytohormones salicylic acid (SA), jasmonic acid (JA), and abscisic acid (ABA). Open arrowheads indicate direct chemical and/or enzymatic links; closed arrowheads indicate indirect links by signaling events. (This figure is available in color at *JXB* online.)

usually visible 3 to 4 h after treatment. Common markers of PCD such as DNA laddering and cytochrome C release from mitochondria were not investigated in the present study. Therefore, more research is needed to define the exact mode of NO_2-induced cell death.

The experimental system introduced here allows for the non-invasive treatment of many plants in parallel, which makes it a useful new tool for probing NO_2-induced defense- and cell death signaling by accession and mutant screens.

Supplementary Data

Supplementary data are available at *JXB* online.
Figure S1. Pre-fumigation with 30 ppm NO or 10 ppm NO_2 promotes NO_2-induced cell death.
Table S1. Mutant lines used in NO_2 fumigation experiments.

Acknowledgements

We thank Johanna Leppälä and Mikael Brosché for donating mutant lines and Michael Reichelt for support with the phytohormone measurements. This work was partly supported by the German Plant Phenotyping Network funded by the German Federal Ministry of Education and Research (DPPN, project identification no. 031A053C).

References

Ahlfors R, Brosché M, Kollist H, Kangasjärvi J. 2009. Nitric oxide modulates ozone-induced cell death, hormone biosynthesis and gene expression in Arabidopsis thaliana. The Plant Journal **58,** 1–12.

Beevers L, Hageman RH. 1969. Nitrate reduction in higher plants. Annual Review of Plant Physiology **20,** 495–522.

Begara-Morales JC, Sánchez-Calvo B, Chaki M, Valderrama R, Mata-Pérez C, Padilla MN, Corpas FJ, Barroso JB. 2016. Antioxidant systems are regulated by nitric oxide-mediated post-translational modifications (NO-PTMs). Frontiers in Plant Science **7,** 152.

Besson-Bard A, Pugin A, Wendehenne D. 2008. New insights into nitric oxide signaling in plants. Annual Review of Plant Biology **59,** 21–39.

Browse J. 2009. Jasmonate passes muster: a receptor and targets for the defense hormone. Annual Review of Plant Biology **60,** 183–205.

Cecconi D, Orzetti S, Vandelle E, Rinalducci S, Zolla L, Delledonne M. 2009. Protein nitration during defense response in Arabidopsis thaliana. Electrophoresis **30,** 2460–2468.

Chiwocha SDS, Cutler AJ, Abrams SR, Ambrose SJ, Yang J, Ross ARS, Kermode AR. 2005. The etr1-2 mutation in Arabidopsis thaliana affects the abscisic acid, auxin, cytokinin and gibberellin metabolic pathways during maintenance of seed dormancy, moist-chilling and germination. The Plant Journal **42,** 35–48.

Crawford NM. 1995. Nitrate: nutrient and signal for plant growth. The Plant Cell **7,** 859–868.

Delledonne M, Xia Y, Dixon RA, Lamb C. 1998. Nitric oxide functions as a signal in plant disease resistance. Nature **394,** 585–588.

de Pinto M, Tommasi F, Gara LD. 2002. Changes in the antioxidant systems as part of the signaling pathway responsible for the programmed cell death activated by nitric oxide and reactive oxygen species in tobacco Bright-Yellow 2 cells. Plant Physiology **130,** 698–708.

Desikan R, Griffiths R, Hancock J, Neill S. 2002. A new role for an old enzyme: nitrate reductase-mediated nitric oxide generation is required for abscisic acid-induced stomatal closure in Arabidopsis thaliana. Proceedings of the National Academy of Sciences of the United States of America **99,** 16314–16318.

Du S, Zhang Y, Lin X, Wang Y, Tang C. 2008. Regulation of nitrate reductase by nitric oxide in Chinese cabbage pakchoi (Brassica chinensis L.). Plant, Cell and Environment **31,** 195–204.

Durner J, Wendehenne D, Klessig DF. 1998. Defense gene induction in tobacco by nitric oxide, cyclic GMP, and cyclic ADP-ribose. Proceedings of the National Academy of Sciences of the United States of America **95,** 10328–10333.

Fancy NN, Bahlmann A-K, Loake GJ. 2016. Nitric oxide function in plant abiotic stress. Plant, Cell and Environment, doi: 10.1111/pce.12707.

Farmer EE, Müller MJ. 2013. ROS-mediated lipid peroxidation and RES-activated signaling. Annual Review of Plant Biology **64,** 429–450.

Frungillo L, Skelly MJ, Loake GJ, Spoel SH, Salgado I. 2014. S-nitrosothiols regulate nitric oxide production and storage in plants through the nitrogen assimilation pathway. Nature Communications **5,** 5401.

Gaupels F, Furch ACU, Zimmermann MR, Chen F, Kaever V, Buhtz A, Kehr J, Sarioglu H, Kogel K, Durner J. 2016. Systemic induction of NO-, redox-, and cGMP signaling in the pumpkin extrafascicular phloem upon local leaf wounding. Frontiers in Plant Science **7,** 154.

Gaupels F, Kuruthukulangarakoola GT, Durner J. 2011. Upstream and downstream signals of nitric oxide in pathogen defence. Current Opinion in Plant Biology **14,** 707–714.

Gilroy S, Suzuki N, Miller G, Choi WG, Toyota M, Devireddy AR, Mittler R. 2014. A tidal wave of signals: Calcium and ROS at the forefront of rapid systemic signaling. Trends in Plant Science **19,** 623–630.

Groß F, Durner J, Gaupels F. 2013. Nitric oxide, antioxidants and prooxidants in plant defence responses. Frontiers in Plant Science **4,** 419.

Ignarro LJ, Fukuto JM, Griscavage JM, Rogers NE, Byrns RE. 1993. Oxidation of nitric oxide in aqueous solution to nitrite but not nitrate: comparison with enzymatically formed nitric oxide from L-arginine. Proceedings of the National Academy of Sciences of the United States of America **90,** 8103–8107.

Joo JH, Wang S, Chen JG, Jones AM, Fedoroff NV. 2005. Different signaling and cell death roles of heterotrimeric G protein alpha and beta subunits in the Arabidopsis oxidative stress response to ozone. The Plant Cell **17,** 957–970.

Katagiri F, Thilmony R, He SY. 2002. The Arabidopsis thaliana-Pseudomonas syringae interaction. The Arabidopsis Book, e0039.

Klepper L. 1979. Nitric oxide (NO) and nitrogen dioxide (NO_2) emissions from herbicide-treated soybean plants. Atmospheric Environment **13,** 537–542.

Kourtchenko O, Andersson MX, Hamberg M, Brunnström A, Göbel C, McPhail KL, Gerwick WH, Feussner I, Ellerström M. 2007. Oxo-phytodienoic acid-containing galactolipids in Arabidopsis: Jasmonate signaling sependence. Plant Physiology **145,** 1658–1669.

Kovacs I, Lindermayr C. 2013. Nitric oxide-based protein modification: formation and site-specificity of protein S-nitrosylation. Frontiers in Plant Science **4,** 137.

Leitner M, Vandelle E, Gaupels F, Bellin D, Delledonne M. 2009. NO signals in the haze. Nitric oxide signalling in plant defence. Current Opinion in Plant Biology **12,** 451–458.

Leon J, Lawton MA, Raskin I. 1995. Hydrogen peroxide stimulates salicylic acid biosynthesis in tobacco. Plant Physiology **108,** 1673–1678.

Levine A, Tenhaken R, Dixon R, Lamb C. 1994. H_2O_2 from the oxidative burst orchestrates the plant hypersensitive disease resistance response. Cell **79,** 583–593.

Lindermayr C, Sell S, Müller B, Leister D, Durner J. 2010. Redox regulation of the NPR1-TGA1 system of Arabidopsis thaliana by nitric oxide. The Plant Cell **22,** 2894–2907.

Liu X, Hou F, Li G, Sang N. 2015. Effects of nitrogen dioxide and its acid mist on reactive oxygen species production and antioxidant enzyme activity in Arabidopsis plants. Journal of Environmental Sciences **34,** 93–99.

Maassen A, Hennig J. 2011. Effect of Medicago sativa Mhb1 gene expression on defense response of Arabidopsis thaliana plants. Acta Biochimica Polonica **58,** 427–432.

Mevius W. 1958. Nitrite. Handbuch der Pflanzenphysiologie **8,** 166–175.

Mignolet-Spruyt L, Xu E, Idänheimo N, Hoeberichts FA, Mühlenbock P, Brosché M, Van Breusegem F, Kangasjärvi J. 2016. Spreading the news: subcellular and organellar reactive oxygen species production and signalling. Journal of Experimental Botany **67,** 3831–3844.

Moreau M, Gyu IL, Wang Y, Crane BR, Klessig DF. 2008. AtNOS/AtNOA1 is a functional Arabidopsis thaliana cGTPase and not a nitric-oxide synthase. Journal of Biological Chemistry **283,** 32957–32967.

Müller S, Hilbert B, Dueckershoff K, Roitsch T, Krischke M, Müller MJ, Berger S. 2008. General detoxification and stress responses are mediated by oxidized lipids through TGA transcription factors in Arabidopsis. The Plant Cell **20,** 768–785.

Mur LAJ, Lloyd AJ, Cristescu SM, Harren FJM, Hall MA, Smith AR. 2008. Nitric oxide interacts with salicylate to regulate biphasic ethylene production during the hypersensitive response. Plant Physiology **148,** 1537–1546.

Mur LAJ, Mandon J, Persijn S, Cristescu SM, Moshkov IE, Novikova G V, Hall MA, Harren FJM, Hebelstrup KH, Gupta KJ. 2013. Nitric oxide in plants: An assessment of the current state of knowledge. AoB Plants **5,** pls052.

Noctor G, Foyer CH. 1998. Ascorbate and glutathione: keeping active oxygen under control. Annual Review of Plant Biology **49,** 249–279.

Oke OL. 1966. Nitrite toxicity to plants. Nature **212,** 528–528.

Overmyer K, Tuominen H, Kettunen R, Betz C, Langebartels C, Sandermann H, Kangasjärvi J. 2000. Ozone-sensitive arabidopsis rcd1 mutant reveals opposite roles for ethylene and jasmonate signaling pathways in regulating superoxide-dependent cell death. The Plant Cell **12,** 1849–1862.

Perazzolli M, Romero-Puertas MC, Delledonne M. 2006. Modulation of nitric oxide bioactivity by plant haemoglobins. Journal of Experimental Botany **57,** 479–488.

Pieterse CMJ, Van der Does D, Zamioudis C, Leon-Reyes A, Van Wees SCM. 2012. Hormonal modulation of plant immunity. Annual Review of Cell and Developmental Biology **28,** 489–521.

Rao M V, Davis KR. 1999. Ozone-induced cell death occurs via two distinct mechanisms in Arabidopsis: The role of salicylic acid. The Plant Journal **17,** 603–614.

Rao M, Lee H, Creelman R, Mullet J, Davis K. 2000. Jasmonic acid signaling modulates ozone-induced hypersensitive cell death. The Plant Cell **12,** 1633–1646.

Romero-Puertas MC, Campostrini N, Matte A, Righetti PG, Perazzolli M, Zolla L, Roepstorff P, Delledonne M. 2008. Proteomic analysis of S-nitrosylated proteins in Arabidopsis thaliana undergoing hypersensitive response. Proteomics **8,** 1459–1469.

Sakamoto A, Sakurao SH, Fukunaga K, Matsubara T, Ueda-Hashimoto M, Tsukamoto S, Takahashi M, Morikawa H. 2004. Three distinct Arabidopsis hemoglobins exhibit peroxidase-like activity and differentially mediate nitrite-dependent protein nitration. FEBS Letters **572,** 27–32.

Sasaki-Sekimoto Y, Taki N, Obayashi T, *et al*. 2005. Coordinated activation of metabolic pathways for antioxidants and defence compounds by jasmonates and their roles in stress tolerance in Arabidopsis. The Plant Journal **44,** 653–668.

Scheler C, Durner J, Astier J. 2013. Nitric oxide and reactive oxygen species in plant biotic interactions. Current Opinion in Plant Biology **16,** 534–539.

Tada Y, Spoel SH, Pajerowska-Mukhtar K, Mou Z, Song J, Wang C, Zuo J, Dong X. 2008. Plant immunity requires conformational charges of NPR1 via S-nitrosylation and thioredoxins. Science **321,** 952–956.

Taki N, Sasaki-Sekimoto Y, Obayashi T, *et al*. 2005. 12-Oxo-phytodienoic acid triggers expression of a distinct set of genes and plays a role in wound-induced gene expression in Arabidopsis. Plant Physiology **139,** 1268–1283.

Taylor OC, Eaton FM. 1966. Suppression of plant growth by nitrogen dioxide. Plant Physiology **41,** 132–135.

Thomas D, Ridnour L, Isenberg J, *et al*. 2008. The chemical biology of nitric oxide: Implications in cellular signaling. Free Radical Biology and Medicine **45,** 18–31.

Torres MA, Dangl JL. 2005. Functions of the respiratory burst oxidase in biotic interactions, abiotic stress and development. Current Opinion in Plant Biology **8,** 397–403.

Vadassery J, Reichelt M, Hause B, Gershenzon J, Boland W, Mithöfer A. 2012. CML42-mediated calcium signaling coordinates responses to Spodoptera herbivory and abiotic stresses in Arabidopsis. Plant Physiology **159,** 1159–1175.

Vanzo E, Merl-Pham J, Velikova V, Ghirardo A, Lindermayr C, Hauck SM, Bernhardt J, Riedel K, Durner J, Schnitzler J-P. 2016. Modulation of protein S-nitrosylation by isoprene emission in poplar. Plant Physiology **170,** 1945–1961.

Wang Y, Loake GJ, Chu C. 2013. Cross-talk of nitric oxide and reactive oxygen species in plant programed cell death. Frontiers in Plant Science **4,** 314.

Xu E, Vaahtera L, Brosché M. 2015. Roles of defense hormones in the regulation of ozone-induced changes in gene expression and cell death. Molecular Plant **8,** 1776–1794.

Yan S, Dong X. 2014. Perception of the plant immune signal salicylic acid. Current Opinion in Plant Biology **20,** 64–68.

Yu M, Lamattina L, Spoel SH, Loake GJ. 2014. Nitric oxide function in plant biology: A redox cue in deconvolution. New Phytologist **202,** 1142–1156.

Yun B-W, Feechan A, Yin M, *et al*. 2011. S-nitrosylation of NADPH oxidase regulates cell death in plant immunity. Nature **478,** 264–268.

Zeevaart AJ. 1976. Some effects of fumigating plants for short periods with NO2. Environmental Pollution **11,** 97–108.